IEEE Access
Multidisciplinary | Rapid Review | Open Access Journal

Received December 23, 2019, accepted January 8, 2020, date of publication January 13, 2020, date of current version January 28, 2020.

Digital Object Identifier 10.1109/ACCESS.2020.2966236

Platoon Separation Strategy Optimization Method Based on Deep Cognition of a Driver's Behavior at Signalized Intersections

JUNJIE CHEN[1] AND JIAN SUN[2,3]

[1]School of Electronics and Information Engineering, Beijing Jiaotong University, Beijing 100044, China
[2]State Key Laboratory for Strength and Vibration of Mechanical Structures, School of Aerospace, Xi'an Jiaotong University, Xi'an 710049, China
[3]Shaanxi Engineering Laboratory for Vibration Control of Aerospace Structures, Xi'an Jiaotong University, Xi'an 710049, China

Corresponding author: Jian Sun (sunjian10@xjtu.edu.cn)

This work was supported in part by the Fundamental Research Funds for the Central Universities under Grant 2018YJS029, and in part by the Department of Mechanical Engineering, Carnegie Mellon University, Pittsburgh, USA.

ABSTRACT Semantic understanding of drivers' behavior features at intersections plays a pivotal role in the proper decision-making of a platoon. This paper presents a flexible framework to automatically extract the driver's driving features from observed temporal sequences of driving raw data and traffic light information. An approach, which contains two key sub-problems, is proposed to select the separated vehicles from the platoon in the vicinity of the intersection. Then, the first sub-problem, accurately capturing the drivers' driving behavior features under the impact of traffic lights, is addressed by using the Bayesian nonparametric approach, which could segment drivers' driving raw data temporal sequences into small analytically interpretable components (called driving primitives) without using prior knowledge. In addition, the extracted driving primitives are used to obtain the vehicle separation strategy (which is also the second sub-problem) by considering safety, efficiency, and energy consumption. Finally, 200 groups of raw data of human-driven vehicles approaching the intersection are used to validate the effectiveness of the proposed primitive-based framework. Experimental results demonstrate that the acceleration indeterminacy of separated vehicles could be decreased 37%-72% by segmenting the captured driving behavior features into 3×15 patterns. Moreover, the vehicle separation strategy could not only increase the efficiency, but also the safety, and the energy consumption could be decreased.

INDEX TERMS Platoon separation, nonparametric Bayes, platoon operating optimization at intersection, increased operating safety and efficiency.

I. INTRODUCTION

Platoon separation scenario in this paper refers to the scenario where multiple vehicles operating in the form of the platoon are spatially close to the intersection [1]–[3]. Since the limited green light duration, some vehicles have to cross the intersection in the next green light phase or separate from the platoon and cross the intersection by moving into other lanes. Vehicle separation is one of the most common driving scenarios [4]–[6] for platoon operating in the vicinity of the intersection, which will increase the platoon number and add communication pressure to the infrastructure [7]. The latest statistical data of the National Highway Traffic Safety Administration (NHTSA) indicates that around 40% of all crashes and 50% of severe collisions in the U.S. occur at intersections [8], which indicates the importance of kepping the intersection traffic scenario safe. Human driving behavior is a dynamic and stochastic process in nature [9]. The road users do not solely determine their behaviors based on their current states but also predict the behaviors of others at intersections [10]. The limited and obscured sight distances and wrong intuition on gap acceptance are the main factors in these accidents [11]. For a platoon, the typical process of negotiating at intersections usually consists of a closed-loop of perception, decision making, and control. Due to uncertainties on the continuous state of nearby vehicles and their potential discrete states such as braking and turning, decision making is becoming the most crucial and challenging component [12]. Thus, in order to make platoon vehicles able to interact with nearby human drivers smoothly and

The associate editor coordinating the review of this manuscript and approving it for publication was Maurice J. Khabbaz.

safely, the platoon intersection driving scenarios should be thoroughly investigated.

Many solutions have been developed to analyze and model the platoon driving behavior at intersections, thus providing essential operating rules for platoons. For example, subjectively decomposing the road in the vicinity of intersection, into finite segments, within each segment, vehicles operate under different control methods [13]. Researchers segment the intersection connected road into three parts (approach area, adjust area and maintain area), and then guide the vehicles by using the double-loop Spatial Position Associating Time Series (SPATS) method and the Acceleration Dynamically Adjusting based on Predicted Trajectory (ADAPT) method [14]. Slot-based intersections, which could replace traditional traffic lights, have also been implemented to reduce queues and delays. However, the approaches mentioned above cannot keep the integrity of the platoon; they require the prior knowledge of, for example, road conditions (e.g., intersection type) and signal information (e.g., signalized and non-signalized traffic), which makes it restricted to some specific conditions. For instance, Tachet et al. implemented a space-time slot model to increase traffic efficiency only at the non-signalized intersection [15]. Sarkar et al. mainly focused on the left turn scenarios of traffic agents at the T-shape intersection [16]. Weiming et al. mainly evaluated the energy consumption of the platoon in the green light phase [17], while Alejandro focused on safety when platoon gets through the intersection by adding the virtual platoon [18]. The approaches aforementioned are suitable to use under specific situations. However, it is practically intractable for complicated scenarios because of insufficient prior knowledge on the interactive driving patterns among the traffic agents.

Recently, some driver feature cognitive methods have been implemented to facilitate the decision-making process of autonomous vehicles. For example, Haneen Farah collected the data on the overtaking behavior of 100 drivers by analyzing the data features. The results show interesting and significant differences in the overtaking behavior of drivers depending on their age and gender [19]. Ilka evaluated the Time to Intersection (TTI) time interval between field and simulator at five simple urban intersections. The braking behavior near urban intersections differs between real and simulated experimental environments for drivers has been proved [20]. Although these methods have been successfully implemented in specific cases, they are still limited to be used to understand the context behind the behaviors and may need tremendous data storage resources. Thus, segmenting driver behavior into recognizable patterns can help us understand the driver's intention, and thereby facilitate computational-cost and storage-cost algorithms to practice, for example, Bayesian nonparametric. This method is a common and ï exible way to model multi-decision problems under uncertainties of the intersection driving patterns by providing a mathematically rigorous framework [21]. However, accurately capturing driver behavior characteristics is computationally intractable, especially for the intersection driving scenarios that contain unknown states and multi-vehicles. Fortunately, both the internal fixed relation between driving behaviors and the impact of the infrastructure on driving behaviors could help to reduce the range of locked driver features. For instance, Wenshuo analyzed the vehicle following data and got the driver's following behavior characteristics [22], because the following behavior exists all the time for two vehicles running in one lane. Since Gipps proposed a deterministic lane-changing model concept based on gap-acceptance, in which a driver's behavior is governed by two primary considerations: maintaining the desired speed or being in the correct lane for an intended turning maneuver [23]. Junjie got the driver's overtaking behavior features by setting three critical parameters based on Gipps's research work [24]. Thus, segmenting complex driving behaviors into discrete patterns can facilitate the decision-making learning process and reduce the computational cost and storage cost, especially for the issues in high dimensional space.

According to the discussion above, it is necessary to develop an approach that can accurately capture drivers' behavior characteristics and semantically decompose the complex interactive driving behavior at intersections into discrete states with less prior knowledge. In addition, uncertainties of the potential behavior feature patterns should be considered. However, the complexity and uncertainty of the driving environment make it hard to find a mathematically rigorous united approach to capture the driving behavior features and analyze the behaviors at all kinds of intersections. Besides, the big traffic data in a high-dimensional and large-scale space will overwhelm the human mind and heuristic analysis [25].

This paper will introduce a primitive-based framework, which can automatically decompose the drivers' driving behavior at intersections into several interpretable patterns with less prior knowledge by integrating Bayesian nonparametric learning algorithms. Also, this method could accurately capture the driver's driving behavior features at the intersection.

Our work focuses on generating platoon separation strategies by considering single human-driven vehicle driver's driving features and making full use of road section resources by selecting the separation vehicles running on other lanes. So that we can consider there is no V2V communication in the platoon(the strategy can be generated by the platoon vehicle or by the infrastructure).

The main contributions of this paper are threefold.

- Presenting a primitive-based framework to learn drivers' driving features at intersections based on Bayesian nonparametric statistics and the impact of the traffic light on driver's driving behavior.
- Developing an efficient vehicle separation strategy for selecting vehicles from the platoon by considering safety, efficiency, and energy consumption.

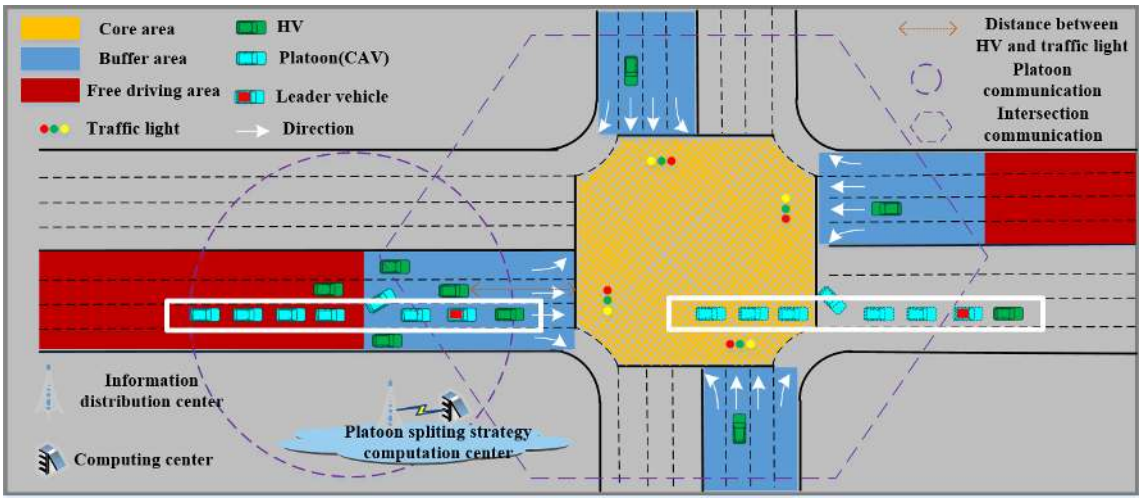

FIGURE 1. Platoon operating in the vicinity of the intersection.

• Verifying the effectiveness of our proposed framework for analyzing drivers' driving behavior features through emulation driving data.

The remainder of this paper is organized as follows. Section 2 introduces the selection process of separated vehicles. Section 3 introduces the developed primitive-based framework. Section 4 introduces the vehicle separation strategy based on safety and energy consumption. Section 5 discusses and analyzes the experimental results. Section 6 concludes this work and discusses future work.

II. VEHICLE SEPARATION SELECTION PROCESS

A platoon is a method of driving multiple vehicles together in a single lane maintaining a safe distance between the vehicles. To cross the intersection within the green light duration, some vehicles separate from the platoon and cross the intersection by using other lanes. However, the motion patterns of human-driven vehicles are unknown as drivers have different driving behaviors at the traffic light, which makes it challenging to select the separated vehicles. Through this paper, we propose a vehicle separation selection process by analyzing the behaviors of drivers operating on the other lanes, at different traffic lights. We also consider vehicle safety and energy consumption. The vehicle separation scenario is shown in Fig. 1, and the vehicle separation selection process is described below.

Step 1: The platoon uploads the raw operating data (position, velocity, acceleration, vehicle number, time headway, and vehicle length). Simultaneously, the infrastructure uploads traffic light information to the computing center(inside the vehicle or the infrastructure), which decides whether the platoon should be allowed to cross the intersection or not.

$$v_p + a_p t_0 = v_p' \le v_1. \tag{1}$$

$$v_p t_0 + \frac{1}{2} a_p t_0^2 + v_p'(t_g - t_0) \ge (n-1) v_p t_1 + \ell + L. \tag{2}$$

where v_p and v_p' represent the velocity and accelerated velocity of the platoon. a_p, t_0, and t_1 represent the acceleration, the acceleration time, and the time headway of the platoon, respectively. L represents the distance between leader vehicle and intersection, v_1 represents the limited road velocity, t_g is the remaining green light duration, n represents the vehicle number of the platoon, and ℓ is the length of the vehicle. If (2) is established, the platoon crosses the intersection by accelerating; otherwise, the platoon separates some vehicles to cross the intersection.

Step 2: Obtain the vehicle separation number n_0.

$$v_p t_0 + \frac{1}{2} a_{max} t_0^2 + v_1(t_g - t_0) \ge (n_1 - 1) v_p t_1 + \ell + L. \tag{3}$$

where a_{max} represents the maximum acceleration, and n_1 represents the maximum number of vehicles that can cross the intersection if the platoon is moving in the original lane, such that the number of separated vehicles is $n_0 = n - n_1$.

Step 3: The raw data (position, velocity, acceleration) of human-driven vehicles (HV) moving in other lanes are uploaded to the computer center, after which the time to the intersection (TTI) of the human-driven vehicle is obtained.

$$TTI = \frac{s_d}{v_{d0}}. \tag{4}$$

where s_d represents the distance between the human-driven vehicle and the intersection, and v_{d0} represents the velocity of the human-driven vehicle.

For the sake of simplicity, this paper assumes that there is just one lane beside the original lane, and the human-driven vehicle number is i and the time to collision between two consecutive cars is TTC.

$$TTC_r = TTI_r - TTI_{r-1}. \tag{5}$$

where r represents the serial number of the human-driven vehicle, and $1 \le r \le i$.

Step 4: Get the range of TTI, velocity, and acceleration of the driver, at the time when the traffic light influences the driver, and then divide the above three parameters into M, N, and Q levels, respectively. Finally, select the thresholds for each parameter.

Step 5: From Step 4, there are $M \times N \times Q$ driving types that represent different driving behaviors. This means that the driver approaches the intersection in the velocity range of $v_k(k \in (1, Q))$, acceleration range of $a_j, (j \in (1, N))$, and within $TTI_\alpha(\alpha \in (1, M))$. By counting the proportion of different driving types, the driver's driving behavioral features can be treated as (TTI_α, a_j, v_k).

Step 6: As vehicles can form lane-changing zones, the separated vehicles from the platoon can overtake or follow the human-driven vehicles in the lane-changing zones. After getting the driving types of the human-driven vehicles, we learn the maximum number of vehicles that can change the lane safely.

$$\begin{cases} Z_1 = q_1, \\ Z_2 = q_2, \\ \cdots\cdots \\ Z_{i+1} = q_{i+1} \end{cases} \tag{6}$$

where Z represents the lane-changing zones and q represents the number of vehicles that can safely move in this zone. If the zone is too short to accept even one vehicle, then $q = 0$.

Step 7: Select the vehicle as a separated vehicle if it has the minimum acceleration for lane changing. In theory, there are $A_n^{n_0}$ cases for selecting the separated vehicles. Assuming that there are corresponding η zones for the above cases, there is,

$$q_1 + q_1 + \cdots + q_\eta \le n_0. \tag{7}$$

$$ca = \min\left(\max(ca_1), \max(ca_2), \cdots, \max(ca_{A_n^{n_0} \times A_{i+1}^{\eta} 6pt})\right) \tag{8}$$

where ca is the vehicle separation selection strategy. There are $A_n^{n_0} \times A_{i+1}^{\eta}$ cases for n_0 separated vehicles operating in η lane-changing zones.

Step 8: Evaluate the energy consumption of each separation strategy as there are several strategies obtained in Step 7. If the maximum acceleration has the same value in each strategy, then the optimized case is the one with the minimum energy consumption.

$$ca = \min EC[ca_1, ca_2, \cdots, ca_{\delta 4pt}] \tag{9}$$

where EC is the energy consumption and δ is the case number obtained in Step 7.

Two issues exist in the process of vehicle separation selection: (1) determining driving style based on the influence of the traffic light and (2) obtaining the optimized vehicle separation strategies after getting the driver's driving style. This paper addresses the two issues in Section 3 and Section 4, respectively.

III. METHOD TO EXTRACT DRIVING PATTERNS

For analyzing the impact of a driver's unknown driving style on the vehicle separation function, this paper sets the traffic parameters as follows: 7 vehicles in the platoon, the velocity of platoon is $10m \cdot s^{-1}$, vehicle length is $5m$, the distance between the leading vehicle and the intersection is $10m$,

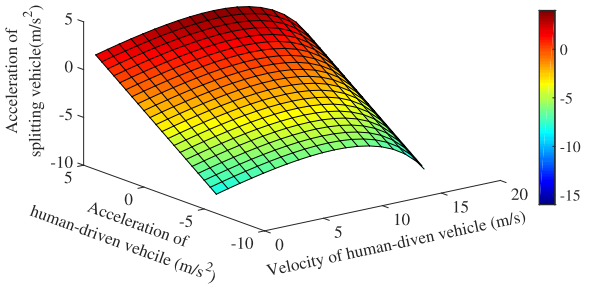

FIGURE 2. Acceleration range of the separated Vehicle when overtaking.

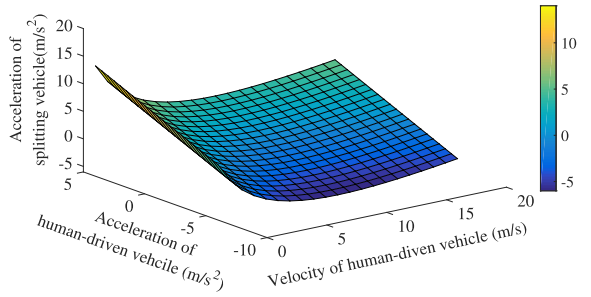

FIGURE 3. Acceleration range of the separated vehicle when following.

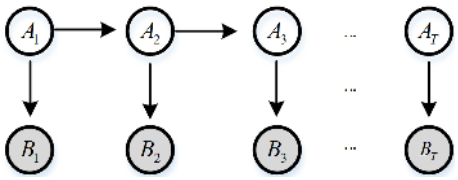

FIGURE 4. Structure of HMM.

the time headway is $2s$, and there is only one vehicle in the other lane moving parallel to the fourth vehicle. The acceleration ranges of vehicle #3 and vehicle #5 are as shown in Fig. 2 and Fig. 3, from which we can get the information, as the vehicle separation has a wide range of acceleration variation, the accurate lane-changing position and operation patterns cannot be obtained.

The human-driven vehicle's approaching the intersection can be broken down into different driving primitives so that the whole driving process is regarded as a combination of a series of different operation primitives. This section will detail three Bayesian nonparametric learning methods, which are influential in modeling driver behavior in the case where the number of primitive driving patterns is not precisely known. In what follows, we present the theoretical basis of the Hidden Markov model (HMM), Hidden Semi-Markov Model (HSMM), and Hierarchical Dirichlet processes (HDP).

A. HMM

The core of HMM consists of two layers: a layer of a hidden state and a layer of observation or emission, as shown in Fig. 4, where the shaded nodes are observations, and the unshaded nodes are latent states [26].

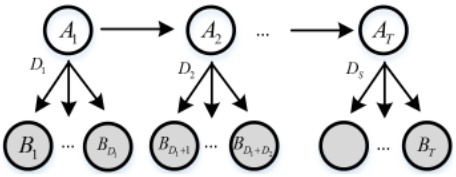

FIGURE 5. Structure of HSMM.

Given a time-series data sequence $B = \{b_t\}_{t-1}^{T}$ and a set of hidden state A, each hidden state A_t at time t will be subject to one entry of A. The transition probability from the hidden state A_i to A_j is denoted as $T_{i,j}$ with $T_i = [T_{i1}, T_{i2}, T_{i3}, \cdots]$. The observation b_t at time t in given hidden state A_t is generated by $B_t = f(B_t|A_t, x_{A_t})$, called the emission function. Therefore, the HMM can be described as

$$A_i|A_{i-1} \sim T_{A_{i-1}}. \tag{10}$$

$$B_t|A_t \sim f(x_{A_t 4pt}). \tag{11}$$

where $f(\cdot)$ is the emission function and $x_{A_t 4pt}$ is the emission parameter.

B. HSMM

The hidden semi-Markov model (HSMM), as an extension of HMM, is traditionally defined by allowing the underlying process to be a semi-Markov chain, which means that each state has a variable duration [27], as shown in Fig. 5.

Several approaches can be used to define HSMM depending on the assumptions and applications. In this paper, we assume that each hidden state's duration is given over an explicit distribution, also called explicit duration HMM. Therefore, we augment the generative process of a standard HMM with a random state duration time, drawn from some a state-specific distribution when the state is entered. Here, we use the random variable d_t to denote the duration of a state that enters at time t, and $p(d_t|A_t = i)$ denotes the probability mass function for d_t. Similar to HMM, we can define HSMM by

$$A_i|A_{i-1} \sim T_{A_{i-1}}. \tag{12}$$

$$d_s = g(\omega_s). \tag{13}$$

$$B_t|A_t \sim f(x_{A_t 4pt}). \tag{14}$$

where $g(\omega_s)$ is a state-specific distribution over the state duration d_s.

C. HDP

Drivers' behaviors, however, are changing and opened, so that the parameter space regarding hidden states in the model becomes potentially infinite. More specifically, the dimension of the set space of hidden states $|A|$, is unknown. In such situations, we have to define a prior probability distribution on an infinite-dimensional space. A distribution on an infinite dimensional space is a stochastic process with a specific path. Usually, the Dirichlet processes (DP) rapidly yield intractable computations. In what follows, we will introduce a hierarchal DP (HDP) [28].

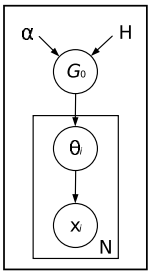

FIGURE 6. Graph model structure of DP.

We assume that the number of latent states is previously unknown and these modes of HMM are subject to a specific distribution defined over a measure space. The Dirichlet process (DP) is a measure on measures, denoted by $DP(\alpha, H)$, and provides a distribution over discrete probability measures with an infinite collection of atoms on a parameter space that is endowed with a base measure H. The Graph model structure of DP is shown in Fig. 6. Here, the weights β_i is sampled by a stick-breaking construction and we denote $\beta \sim GEM(\gamma)$, with $\beta = [\beta_1, \beta_2, \beta_3, \cdots]$ and $\sum_{i=1}^{\infty} \beta_i = 1$.

$$G_0 = \sum_{i=1}^{\infty} \beta_i \delta_{\theta_i}, \ \theta \sim H. \tag{15}$$

$$\beta_i = v_i \prod_{\ell=1}^{i-1} (\ell - v_\ell), \ v_i \sim Beta(1, \gamma). \tag{16}$$

According to the above discussion, an HDP can be used to define a prior state on the set of HMM transition probability measures $G_{j,i}$.

$$G_{j,i} = \sum_{i=1}^{\infty} T_{j,i} \delta_{\theta_i}. \tag{17}$$

where δ_{θ_i} is a mass concentrated at θ. Assuming that each discrete measure G_j is a variation on a global discrete measure G_0, thus the Bayesian hierarchical specification takes $G_j \sim DP(\alpha, G_0)$, where G_0 is draw from $DP(\gamma, H)$.

$$G_0 = \sum_{i=1}^{\infty} \beta_i \delta_{\theta_i}, \ \beta|\gamma \sim GEM(\gamma). \tag{18}$$

$$G_j = \sum_{i=1}^{\infty} T_{j,i} \delta_{\theta_i}, \ T_j|\alpha, \beta \sim DP(\alpha, \beta). \tag{19}$$

D. STICKY HDP-HMM

For the sticky HDP-HMM (γ, α, H), adding an extra parameter $\kappa > 0$ [29] biases the process toward self-transition in (19) and increases the expected probability of self-transition by an amount proportional to κ. The graphic illustration is shown in Fig. 8; therefore, we can obtain

$$T_i|\alpha, \beta, \kappa \sim DP(\alpha + \kappa, \frac{\alpha\beta + \kappa\delta_i}{\alpha + \kappa}). \tag{20}$$

All the hyperparameters are set as a Gamma distribution for the convenience of estimating the posterior probability

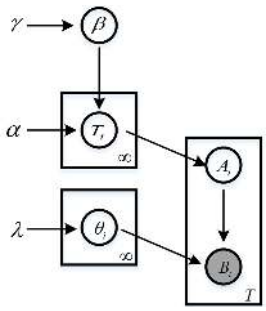

FIGURE 7. Structure of HDP-HMM.

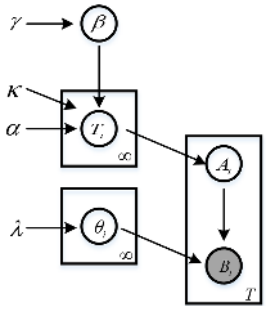

FIGURE 8. Structure of Sticky HDP-HMM.

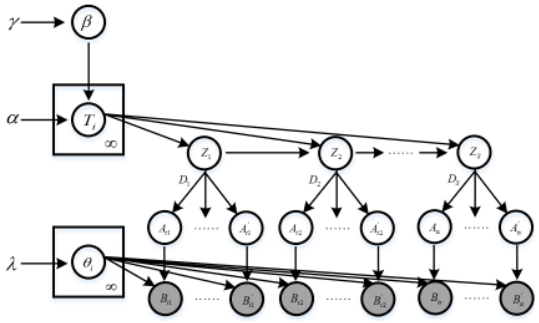

FIGURE 9. Structure of HDP-HSMM.

of hidden states, and this method has been proved in [22]. Based on the above discussion, by applying the HDP prior to the HMM and HSMM, we can obtain the HDP-HMM, sticky HDP-HMM, and HDP-HSMM, as shown in Figs. 7-9.

IV. SEPARATION STRATEGY UNDER SEC REQUIREMENTS

The optimized vehicle separation strategy should maintain the separated vehicle's safety and efficiency. Also, the remaining vehicles in the platoon should have minimum energy consumption. In this paper, we call these SEC (Safety, Efficiency, and Energy consumption) requirements.

The platoon can predict the human-driven vehicle's behavior after the drivers' driving features are obtained. It is necessary to study the secure condition of lane-changing, the capacity of lane changing area for the separated vehicles, and the restrictions of obtaining the optimized vehicle separation strategies. The next section will address the above three issues in detail.

A. SAFE FOLLOWING DISTANCE BETWEEN THE TWO VEHICLES

In this study, we assume that v_r and v_{pr} denote the velocity of the rear vehicle and the preceding vehicle, respectively. The distance between the two vehicles is H. a_0 and a_1 denote the maximum deceleration of the rear vehicle and the preceding vehicle, respectively. t_3 denotes the reaction time of the driver, and t_4 denotes the time of deceleration increase. Once the vehicles stop, the safe distance between the two vehicles should be larger than ℓ_1.

Two velocity relationships exist between the preceding vehicle and the rear vehicle:

(1) The velocity of the rear vehicle is equal or greater than that of the preceding vehicle.

$$H_1 = v_r t_3 + \frac{v_r^2}{2a_0} - \frac{v_{pr}^2}{2a_1} + \int_0^{t_4} \left((v_r - v_{pr}) + (\frac{a_1 - a_0}{2t_4}) \cdot t^2\right) dt + \ell_1 \quad (21)$$

(2) The velocity of the rear vehicle is less than that of the preceding vehicle.

$$H_2 = v_r t_4 + \frac{v_r}{a_1}\left(v_{pr} - v_r - \int_0^{t_4} \frac{a_1}{t_4} t dt\right) + H_1 \quad (22)$$

For safety, the distance between the rear vehicle and the preceding vehicle should larger than H_1 or H_2 under the corresponding velocity relationship.

B. THE CAPACITY OF LANE CHANGE AREA FOR THE SEPARATED VEHICLES

When computing the capacity of the lane changing area for the separated vehicles, the safety lane-changing conditions in Section A should be fully considered. This means that the vehicle separation should keep the safety distance with the human-driven vehicle after changing the lane. Also, when several vehicles change the lane and enter the same lane-changing zone, a safety following slot should be kept. Most importantly, the state of human-driven vehicles should not be impacted by the separated vehicle.

For the sake of simplicity, this paper assumes that there is only one human-driven vehicle in the other lane, so that two lane-changing zones are formed. Set the driver's driving style to (TTI_d, a_d, v_d) when approaching the intersection. To maintain the vehicle's safety after separation, the overtaking velocity is $v_s \geq v_d$, or the following velocity is $v_s \leq v_{d0}$.

The separated vehicles should keep a safe distance from the preceding vehicle after overtaking the human-driven vehicle.

$$H_1(v_d, v_s) + (n_x - 1)H_1(v_s, v_s) \leq s_d \quad (23)$$

The capacity of the lane changing zone in the downstream of human-driven vehicle is

$$n_x \leq \frac{s_d - H_1(v_d, v_s)}{H_1(v_s, v_s)} + 1 \quad (24)$$

When the separated vehicles follow the human-driven vehicle, all the separated vehicles should cross the intersection in the green light duration.

$$\frac{H_2(v_s, v_{d0})}{v_s} + (n_s - 1)\frac{H_1(v_s, v_s)}{v_s} \leq t_r \tag{25}$$

where t_r represents the remaining green light duration after the human-driven vehicle crosses the intersection.

$$t_r = t_g - (\frac{s_d}{v_{d0}} - TTI_d) - \frac{v_d - v_{d0}}{a_d} - \frac{TTI_d \cdot v_{d0} - \frac{(3v_d - v_{d0})(v_d - v_{d0})}{2a_d}}{v_d} \tag{26}$$

so that the capacity of lane changing zone in the upstream of the human-driven vehicle is

$$n_s \leq \frac{t_r v_s - H_2(v_s, v_{d0})}{H_1(v_s, v_s)} + 1 \tag{27}$$

C. THE OPTIMIZED STRATEGY FOR THE VEHICLE SEPARATION OPERATION

After getting the safety lane-changing conditions, we obtain the capacity of lane change area for the separated vehicles, the serial number of the separated vehicles, and the safety velocity v_p^h,($p = 1, 2, \cdots, n_0$, it is the serial number of the separated vehicle. $h = 1, 2, \cdots, i + 1$, it is the serial number of the lane-changing zone) for the separated vehicle running in the lane-changing zone. Setting the acceleration time as t_a for the separated vehicle when changing the lane, the acceleration of the separated vehicle running in the lane-changing zone is as follows:

$$a_h = \frac{v_p^h - v_s}{t_a} \tag{28}$$

The optimized acceleration is $\min|a_h|$ for the separated vehicle. The optimized lane-changing zone is the one that has the minimum acceleration. When computing the minimum acceleration of the separated vehicle, there are several optimized results. This means that the optimized accelerations are the same for the different separated vehicles, such that, when selecting the separated vehicles, the energy consumption of the remaining vehicles in the platoon is to be considered.

Li-Min *et al.* [30] has leveraged the numerical simulation method to study the aerodynamic characteristics of a serial vehicle platoon in the intelligent transport system. Fig. 10 shows the variation of the drag coefficient of the car with the number of vehicles in the platoon at a fixed distance. At a fixed interval, as the number of vehicles in the platoon increases, the drag coefficient of each vehicle is continuously decreasing, and the maximum reduction is nearly 40%, but the reduction is significantly low. The resistance of the subsequent vehicles is generally lower than that of the previous vehicles. However, as the number increases, the car with the lowest resistance is roughly at the center of the platoon. The analysis results for the platoon with seven vehicles showed that the vehicle with the lowest drag coefficient was at the center of the platoon, i.e., the fourth vehicle had the lowest

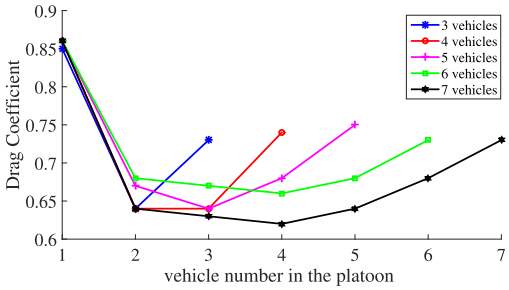

FIGURE 10. Drag coefficients of vehicles in different platoon.

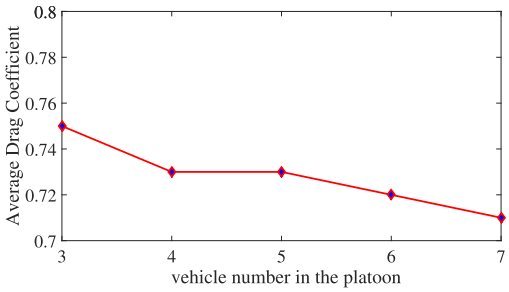

FIGURE 11. Average drag coefficients of platoon with different size.

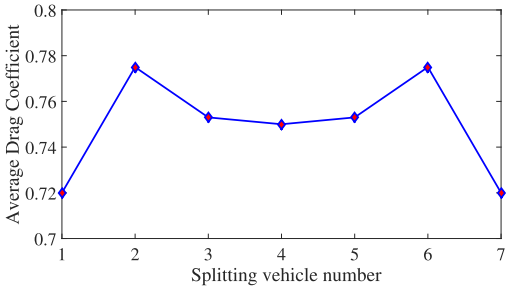

FIGURE 12. Average drag coefficient of the remaining vehicles after separation.

drag coefficient. From the results of the average drag coefficient of the platoon in Fig. 11, the average drag coefficient of the platoon is much smaller than that of the single vehicle, and the average drag coefficient is reduced by 20% - 30%. The platoon operating mode significantly reduces fuel consumption and exhaust emissions. Selecting the optimized vehicle separation by comparing the drag coefficients of the remaining vehicles in the platoon.

$$S = \min(dc(\sharp 1), dc(\sharp 2), \cdots, dc(\sharp \Re)) \tag{29}$$

where S represents the serial number of the separated vehicles, $dc(\cdot)$ represents the drag coefficients of the remaining vehicles in the platoon, and $\Re$ is the number of separated vehicles that have the same optimized acceleration.

Fig. 12 shows the average drag coefficient of the platoon after the separated vehicle moves out, and can be used to select the optimized vehicle separation strategy.

V. DATA PREPROCESSING AND PARAMETERS SETTING

The real test site has the properties of a high cost, limited scenarios, and a long construction period. To address the above issues, a virtual test was carried out [31]. We established an

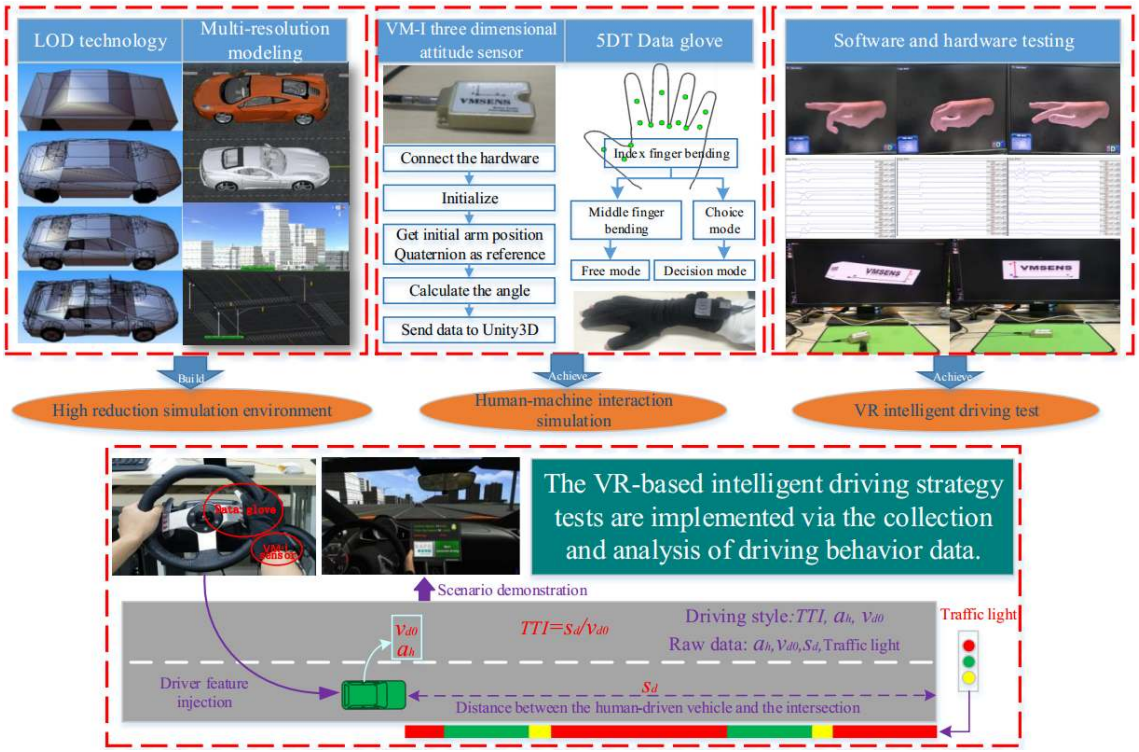

FIGURE 13. The structure diagram of VR based test platform.

interactive intelligent driving simulation platform in a virtual reality environment, as shown in Fig. 13, which realizes a high realistic interactive intelligent driving simulation experience. A virtual reality (VR) based test platform provides a safer and time-saving test option for an autonomous vehicle before a real physical testbed.

The VR based test platform consists of two parts: a high realistic simulation environment and an interactive human driver interface. A three-dimensional real-time simulation environment is implemented, which covers the road network, urban elements, and vehicles. The Logitech G27 racing steering wheel series hardware is used to achieve high immersion intelligent driving. With the VM-I inertial sensor and 5DT data glove, information about the driver's arm that operates the vehicle is dynamically collected in real-time. A communication delay model is used to simulate the information interactive process between vehicles. A series of high-fidelity driving scenarios are implemented, including multiple driving behaviors and multiple intelligent level vehicles.

The influence of the communication quality on the test result is taken into consideration. Furthermore, an SQL database provides the services for the real-time drivers' multi-scene driving behavior data.

The application of the intelligent driving visual simulation platform in this virtual environment can be summarized as the following three aspects: Firstly, providing an online low-cost test environment for an autonomous vehicle; secondly, providing intelligent driving data acquisition and analysis methods for developers; finally, it can also provide a high immersion training platform for drivers.

To generate the data of drivers' driving behavior when approaching an intersection, 20 drivers(8 females and 12 males) were selected to drive in the VR simulation platform. They have different driving experiences, and the driving time varies from 6 months to 10 years. In the intersection scenario, the human-driven vehicle is running on the two-lane one-way road, the initial distance between the ego vehicle and the signalized intersection is 300 meters. The human-driven vehicle expects to cross the intersection, and at the same time, we observe what driving behaviors the driver will do under the influence of traffic lights. This paper repeated the experiment 20 times for each driver in the same settings. Since our work focus on the proposed method, which can get the driver's driving features from the generated raw data, so that the amount of simulation data does not affect the correctness of the method. The data format is shown in Table 1.

This paper got the driving primitives of a human-driven vehicle approaching the intersection by using HDP-HMM, Sticky HDP-HMM, and HDP-HSMM methods. Fig. 14 shows the raw data of one vehicle moving in the vicinity of the intersection, the classification results of driving primitives, and the signal timing scheme in the simulation experiment. In this experiment, the human-driven vehicle approaches the intersection with a distance of 260 meters. When the signal light changed from green to yellow, the velocity of the human-driven vehicle was constant and the acceleration was 0. Once the signal light changed to red, the vehicle slowed down and came to a stop.

The most important thing to the platoon is to obtain the driver's driving behavior before the signal light changes from

TABLE 1. Raw data of HV approaching the intersection.

Velocity $(m \cdot s^{-1})$	Acceleration $(m \cdot s^{-2})$	Distance from intersection(m)	Traffic Signal
11.04266	-1.0716	106.9754	Green
10.9355	-1.0736	105.6649	Green
10.82814	-1.0649	104.7998	Green
10.72165	-1.0569	103.515	Green
8.228373	-5.6199	95.1522	Green
3.166385	0.7226	94.642	Green
3.238645	0.90641	94.3441	Green
3.329286	-9.6308	93.9601	Green
2.166204	-7.38362	93.6132	Green
1.427842	-3.20831	93.3342	Green
1.107011	-2.35686	93.1259	Green
0.871325	-0.42076	92.9701	Green
...	...	...	...

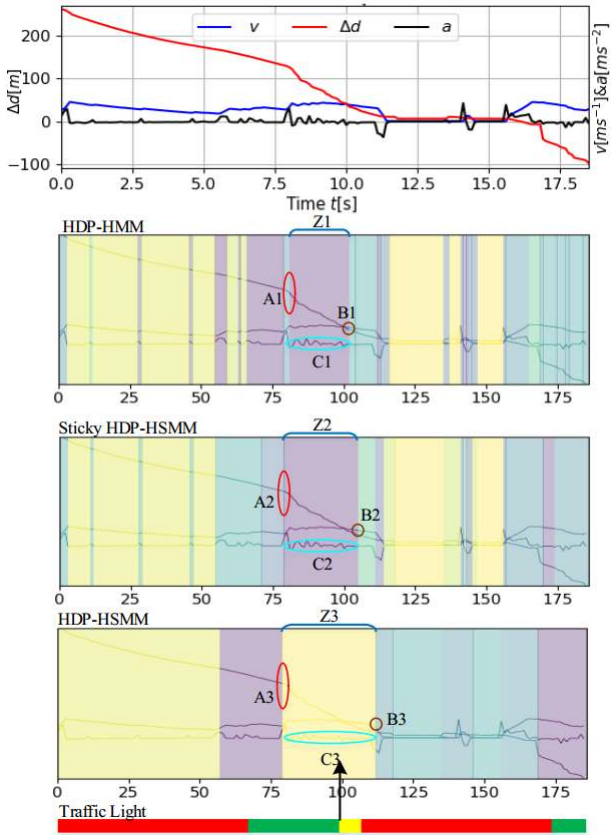

FIGURE 14. Driving primitive obtained by leveraging three methods.

green to yellow. This means that the information about what the human-driven vehicle will do at that specific moment must be obtained. Only by getting this information does the vehicle separation formulate a separation strategy. From Fig. 14, we can get that, the primitive when the signal light changes from green to yellow represents the influence of the signal light on the driver. By using the three Bayesian nonparametric learning methods, the driving primitive

TABLE 2. Variable segmentation.

variable	Variable state	Threshold
Time to intersection(s)	Long time(LT)	> 9.12
	Normal time(NT)	$[2.26, 9.12]$
	Short time(ST)	< 2.26
Velocity$(m \cdot s^{-1})$	Rapidly crossing(RC)	> 22.4
	Gentle crossing(GC)	$[7.86, 22.4]$
	No crossing(NC)	< 7.86
Acceleration$(m \cdot s^{-2})$	Aggressive acceleration(AA)	> 2.41
	Gentle acceleration(GA)	$[0.66, 2.41]$
	No acceleration(NA)	$[-0.4, 0.66]$
	Gentle deceleration(GD)	$[-4.79, -0.4]$
	Aggressive deceleration(AD)	$< -4.79]$

zones(Z1, Z2, and Z3) can be obtained, as shown in the blue brackets.

We can determine the velocity of the human-driven vehicle and the distance between the human-driven vehicle and the intersection from the left boundary of the primitive, as shown by the red circles. Only by using these two parameters can we get the *TTI* value. Also, we can attain the velocity value from the right boundary of the primitive.

From Fig. 14, we can know that by using the three Bayesian nonparametric learning methods, the driver's stress response moments are the same under the influence of the signal light, which proves that our model is reliable, and the driver's stress response behavior exists in the real world, as shown by the red circles. Also, compared with the Sticky HDP-HMM and HDP-HMM, HDP-HSMM method can help us obtain the less short duration driving primitives, which cannot be used to represent the driving features. In summary, this paper gets the driving primitives by using the HDP-HSMM method; the statistical results of approaching intersection features parameters are in Table 2.

By classifying the driver's driving feature parameters, we can get the driver's driving style of approaching the intersection. For each *TTI*, there are 15 kinds of driving styles.

$$\psi(m) = \frac{\phi^m_{ij,k}}{\sum_{i,j} \phi^m_{ij,k}}, \quad (i \in \bigwedge v, j \in a, k \in TTI) \tag{30}$$

where m represents the serial number of the drivers, $\psi(m)$ represents the driver's driving style. i, j, k represent the acceleration, velocity, and the *TTI*, respectively. $\phi^m_{ij,k}$ represents the quantity of driving style of i, j under one kind of *TTI*. The driving style probability distributions of four drivers are shown in Figs. 15-17.

Figs. 15-17 show examples of the normalized frequency distributions of primitive driving patterns for four drivers. Green indicates that the driver has a higher probability of acting in the particular pattern, and dark blue indicates that the driver has a lower probability (nearly equal to zero) of driving in the pattern. For instance, when approaching the

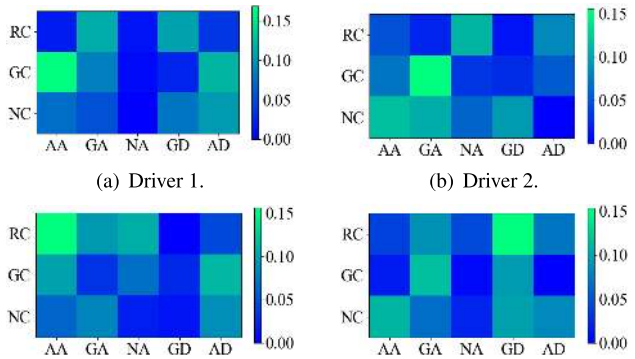

(a) Driver 1. (b) Driver 2.

(c) Driver 3. (d) Driver 4.

FIGURE 15. Driver's driving Style Probability in LT(Long Time) pattern.

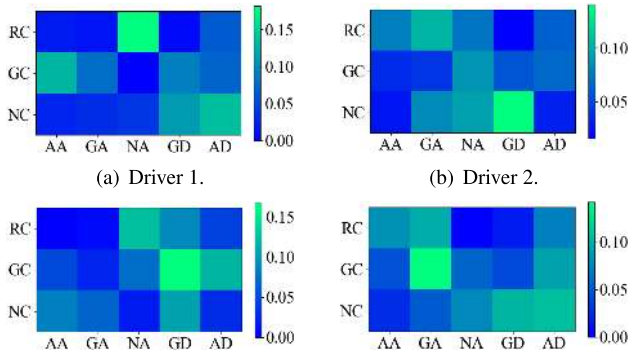

(a) Driver 1. (b) Driver 2.

(c) Driver 3. (d) Driver 4.

FIGURE 16. Driver's driving Style Probability in NT(Normal Time) pattern.

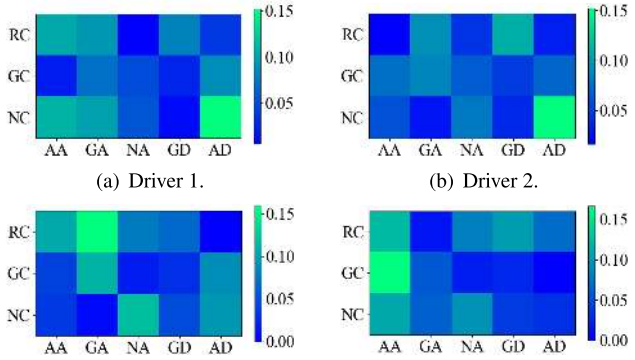

(a) Driver 1. (b) Driver 2.

(c) Driver 3. (d) Driver 4.

FIGURE 17. Driver's driving Style Probability in ST(Short Time) pattern.

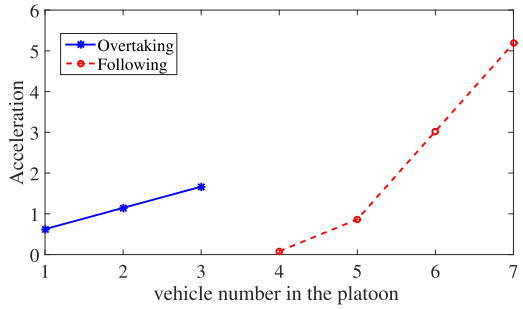

(a) Driver 1 pattern.

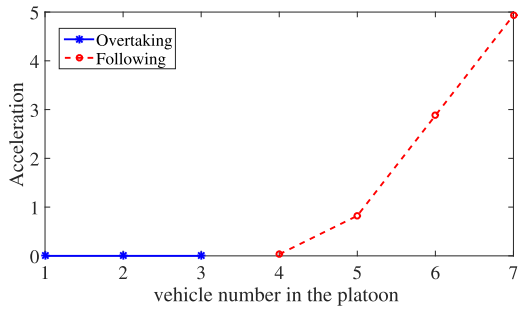

(b) Driver 2 pattern.

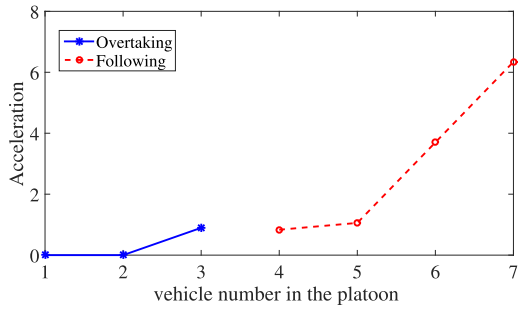

(c) Driver 3 pattern.

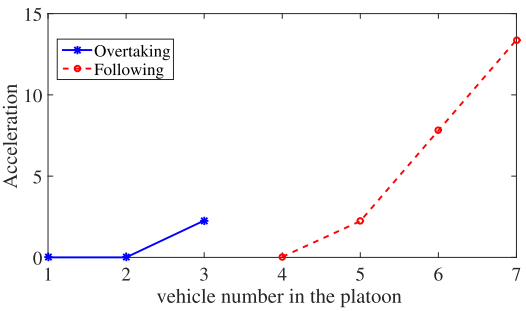

(d) Driver 4 pattern.

FIGURE 18. Acceleration of separated vehicle under different Driver patterns.

intersection in the long-time pattern (Fig. 15), driver 1 and driver 2 prefer to cross the intersection within the general crossing velocity, while driver 3 and driver 4 prefer to cross the intersection rapidly. Additionally, drivers 1, 2, 3 prefer to cross the intersection with the aggressive acceleration or gentle acceleration, which means these drivers have a higher velocity when approaching closer to the intersection. However, driver 4 likes to accelerate the vehicle to a very high velocity, then slow down and cross the intersection. When approaching the intersection in the short time pattern (Fig. 17), drivers 1 and 2 prefer to stop in front of the intersection by aggressive deceleration (the separated vehicle can only overtake these vehicles to cross the intersection), while drivers 3 and 4 prefer to rapidly cross the intersection with the aggressive acceleration or gentle acceleration (the separated vehicle could both overtake and follow the human-driven vehicle to cross the intersection). When approaching the intersection in the normal time pattern (Fig. 16), our

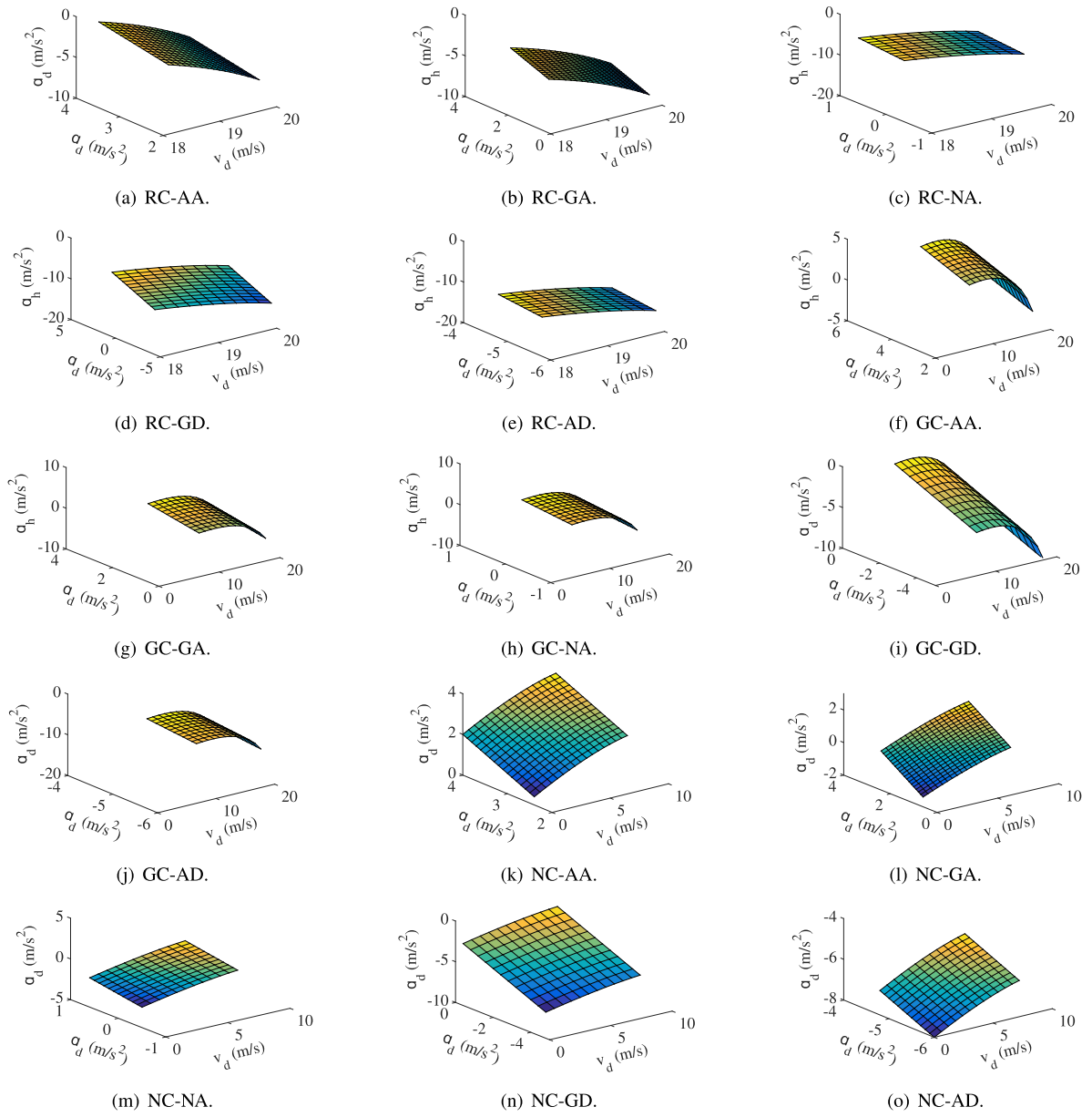

FIGURE 19. Acceleration range of the separated vehicle with the established driving style.

proposed approaches can also provide an intuitive explanation for researchers.

Assuming that there is a platoon operating on the road with seven vehicles in it, the vehicle length is 5 meters, and the time headway is 1 s, the velocity of the platoon is $20m \cdot s^{-1}$, the remaining green signal light duration is 5s, and the position of the human-driven vehicle is parallel to the fourth vehicle of the platoon. Fig. 18 shows the acceleration of separated vehicle (set each vehicle as the separated vehicle) when approaching the intersection, interactive with the four drivers whose driving style is described above. If all vehicles have different accelerations, then the vehicle with the minimum acceleration should be selected as the separated vehicle (for instance, when interacting with driver 1, vehicle #4 should be selected as the separated vehicle). Once more than two vehicles have the same acceleration, for instance, vehicle #1(leader vehicle), #2, #3, and #4 have the same accelerations when interacting with driver 2, the average drag coefficient is used to select the separated vehicle. For the above instance, vehicle #1 should be selected as the separated vehicle since it has the minimum platoon drag coefficient according to Fig. 12.

The platoon should predict the driver's driving style before selecting the separated vehicles. The traffic parameters are set as discussed in section 3; the acceleration range of the separated vehicles(a_h) with the obtained driving style(a_d and v_d) is shown as Fig. 19, from which a comparison is made with the situations where the driver's driving style is unknown, and

the acceleration variation range of the separated vehicles is reduced by an average of 37%–72%.

VI. CONCLUSION

This paper provided a platoon vehicle separation approach with unsupervised learning to learn the driving patterns of the human-driven vehicle at intersections with SEC requirements to select the optimized separation strategy. The Bayesian nonparametric learning was employed to segment the drivers' driving raw data into driving primitives, and selecting the separated vehicle by considering the safety, efficiency, and energy consumption. Experiment results from simulation driving data indicate that the human driving patterns at intersections could be decomposed into finite kinds of semantically interpretable groups. We investigated the distributions of driving primitives of several drivers, which demonstrated that the distribution of human driving patterns could be used as an indicator to identify the types of approaching the signalized intersection. Furthermore, the SEC requirements could help to select the optimized separation strategy. The platoon vehicle separation approach presented in this paper is suitable to select the separated vehicle to guarantee all the platoon vehicles cross the signalized intersection in the green light duration. Although just another one lane is considered because of the limitation of data, our proposed algorithm could be easily extended to the multi-lane signalized intersections, which will be part of our future research.

The Bayesian nonparametric method developed in this paper is based on a mathematically rigorous framework, which can be used to analyze other raw driving data such as the following behavior and overtaking behavior data. The SEC requirements considered the aspects of safety, efficiency, and energy consumption, which can be used to select the optimized vehicle operating strategies. The collected data in this paper only consists of the two-lane one-way signalized intersection. Hence, our future work will be articulated around two axes. The first one is to extend the developed method to the multi-lane intersection. In this way, more features of vehicles presenting at intersections can be extracted, thus allowing us to take further analysis of complex interactions among road users. The second objective is to consider other factors that could impact interactions between human drivers, such as weather, traffic light, and intersection types. Semantically understanding the drivers' driving patterns at signalized intersections could provide a set of recognizable discrete states about complex dynamic systems, thereby helping decision-making design to guarantee traffic efficiency; SEC requirements could provide an essential criterion to select the optimized strategies.

REFERENCES

[1] Y. Feng, D. He, and Y. Guan, "Composite platoon trajectory planning strategy for intersection throughput maximization," *IEEE Trans. Veh. Technol.*, vol. 68, no. 7, pp. 6305–6319, Jul. 2019.

[2] W. Chen, Y. Liu, X. Yang, Y. Bai, Y. Gao, and P. Li, "Platoon-based speed control algorithm for ecodriving at signalized intersection," *Transp. Res. Rec.*, vol. 2489, no. 1, pp. 29–38, Jan. 2015.

[3] L. Shen, R. Liu, Z. Yao, W. Wu, and H. Yang, "Development of dynamic platoon dispersion models for predictive traffic signal control," *IEEE Trans. Intell. Transp. Syst.*, vol. 20, no. 2, pp. 431–440, Feb. 2019.

[4] B. R. Mcauliffe and M. Ahmadi-Baloutaki, "A wind-tunnel investigation of the influence of separation distance, lateral stagger, and trailer configuration on the drag-reduction potential of a two-truck platoon," *SAE Int. J. Commer. Veh.*, vol. 11, no. 2, pp. 125–150, Aug. 2018.

[5] L.-H. Li, J. Gan, and W.-Q. Li, "A separation strategy for connected and automated vehicles: Utilizing traffic light information for reducing idling at red lights and improving fuel economy," *J. Adv. Transp.*, vol. 2018, pp. 1–10, Jul. 2018.

[6] R. D. Cruz-Morales, M. Velasco-Villa, and A. Rodriguez-Angeles, "Chain formation control for a platoon of robots using time-gap separation," *Int. J. Adv. Robot. Syst.*, vol. 15, no. 2, Mar. 2018, Art. no. 172988141877085.

[7] M. Bashiri and C. H. Fleming, "A platoon-based intersection management system for autonomous vehicles," in *Proc. IEEE Int. Veh. Symp. (IV)*, Redondo Beach, CA, USA, Jun. 2017, pp. 667–672.

[8] *Fatality Analysis Reporting System Encyclopedia*, NHTSA, Washington, DC, USA, 2018. Accessed: 2018.

[9] M. Nechyba and Y. Xu, "Stochastic similarity for validating human control strategy models," *IEEE Trans. Robot. Autom.*, vol. 14, no. 3, pp. 437–451, Jun. 1998.

[10] O. Grembek, A. Kurzhanskiy, A. Medury, P. Varaiya, and M. Yu, "Making intersections safer with I2V communication," *Transp. Res. C, Emerg. Technol.*, vol. 102, pp. 396–410, May 2019.

[11] J. I. Creaser, M. E. Rakauskas, N. J. Ward, J. C. Laberge, and M. Donath, "Concept evaluation of intersection decision support (IDS) system interfaces to support drivers gap acceptance decisions at rural stop-controlled intersections," *Transp. Res. F, Traffic Psychol. Behav.*, vol. 10, no. 3, pp. 208–228, May 2007.

[12] W. Schwarting, J. Alonso-Mora, and D. Rus, "Planning and decision-making for autonomous vehicles," *Annu. Rev. Control Robot. Auton. Syst.*, vol. 1, no. 1, pp. 187–210, May 2018.

[13] L. Chai, B. Cai, W. Shangguan, J. Wang, and H. Wang, "Connected and autonomous vehicles coordinating approach at intersection based on space-time slot," *Transportmetrica A, Transp. Sci.*, vol. 14, no. 10, pp. 929–951, Nov. 2018.

[14] L. Chai, B. Cai, W. Shangguan, J. Wang, and H. Wang, "Basic simulation environment for highly customized connected and autonomous vehicle kinematic scenarios," *Sensors*, vol. 17, no. 9, p. 1938, Aug. 2017.

[15] R. Tachet, P. Santi, S. Sobolevsky, L. I. Reyes-Castro, E. Frazzoli, D. Helbing, and C. Ratti, "Revisiting street intersections using slot-based systems," *PLoS ONE*, vol. 11, no. 3, Mar. 2016, Art. no. e0149607.

[16] G. S. Aoude, V. R. Desaraju, L. H. Stephens, and J. P. How, "Driver behavior classification at intersections and validation on large naturalistic data set," *IEEE Trans. Intell. Transp. Syst.*, vol. 13, no. 2, pp. 724–736, Jun. 2012.

[17] W. Zhao, D. Ngoduy, S. Shepherd, R. Liu, and M. Papageorgiou, "A platoon based cooperative eco-driving model for mixed automated and human-driven vehicles at a signalised intersection," *Transp. Res. C, Emerg. Technol.*, vol. 95, pp. 802–821, Oct. 2018.

[18] A. I. Morales Medina, N. Van De Wouw, and H. Nijmeijer, "Cooperative intersection control based on virtual platooning," *IEEE Trans. Intell. Transp. Syst.*, vol. 19, no. 6, pp. 1727–1740, Jun. 2018.

[19] H. Farah, "Age and gender differences in overtaking maneuvers on two-lane rural highways," *Transp. Res. Rec.*, vol. 2248, no. 1, pp. 30–36, Jan. 2011.

[20] I. Zöller, B. Abendroth, and R. Bruder, "Driver behaviour validity in driving simulators—Analysis of the moment of initiation of braking at urban intersections," *Transp. Res. F, Traffic Psychol. Behav.*, vol. 61, pp. 120–130, Feb. 2019.

[21] W. Zhang and W. Wang, "Learning V2V interactive driving patterns at signalized intersections," *Transp. Res. C, Emerg. Technol.*, vol. 108, pp. 151–166, Nov. 2019.

[22] W. Wang, J. Xi, and D. Zhao, "Driving style analysis using primitive driving patterns with Bayesian nonparametric approaches," *IEEE Trans. Intell. Transp. Syst.*, vol. 20, no. 8, pp. 2986–2998, Aug. 2019.

[23] P. Gipps, "A model for the structure of lane-changing decisions," *Transp. Res. B, Methodol.*, vol. 20, no. 5, pp. 403–414, Oct. 1986.

[24] C. Jun-Jie, W. ShangGuan, C. Bai-Gen, J. Wang, and C. Lin-Guo, "Communication block slot optimization method based on intelligent vehicle platoon cognitive ability enhancement," *China J. Highw. Transp.*, vol. 32, no. 6, pp. 283–292, Jun. 2019.
[25] W. Wang, C. Liu, and D. Zhao, "How much data is enough? A statistical approach with case study on longitudinal driving behavior," *IEEE Trans. Intell. Veh.*, vol. 2, no. 2, pp. 85–98, Jun. 2017.
[26] L. R. Rabiner, "A tutorial on hidden Markov models and selected applications in speech recognition," *Proc. IEEE*, vol. 77, no. 2, pp. 257–286, Feb. 1989.
[27] M. J. Johnson and A. S. Willsky, "Bayesian nonparametric hidden semi-Markov models," *J. Mach. Learn. Res.*, vol. 14, pp. 673–701, Feb. 2013.
[28] Y. W. Teh, M. I. Jordan, M. J. Beal, and D. M. Blei, "Hierarchical Dirichlet processes," *J. Amer. Stat. Assoc.*, vol. 101, no. 476, pp. 1566–1581, Dec. 2006.
[29] E. Fox, E. B. Sudderth, M. I. Jordan, and A. S. Willsky, "Bayesian nonparametric inference of switching dynamic linear models," *IEEE Trans. Signal Process.*, vol. 59, no. 4, pp. 1569–1585, Apr. 2011.
[30] F. Li-Min, W. Yun-Zhu, and H. Bao-Qin, "Aerodynamic characteristics of vehicle platoon," *J. Jilin Univ.*, vol. 36, no. 6, pp. 871–875, Nov. 2006.
[31] W. Shangguan, Y. Du, and L. Chai, "Interactive perception-based multiple object tracking via CVIS and AV," *IEEE Access*, vol. 7, pp. 121907–121921, 2019.

JUNJIE CHEN received the B.S. degree from Yanshan University, Hebei, China, in 2013. He is currently pursuing the Ph.D. degree with the School of Electronic and Information Engineering, Beijing Jiaotong University. From 2018 to 2020, he was a Visiting Scholar with Safe AI Lab, Carnegie Mellon University. His research concentrates on cooperative vehicle infrastructure systems of China (CVIS-C), vehicle operational control of CVIS, CVIS modelling and simulation.

JIAN SUN received the Ph.D. degree from Northwest Polytechnical University, in 2007. From 2007 to 2009, he was Postdoctoral Researcher with Tsinghua University, and he entered into Xi'an Jiaotong University, in 2010. From December 2018 to December 2019, he was a Visiting Scholar with Carnegie Mellon University. He is currently an Associate Professor with Xi'an Jiaotong University.